

Book of Tutorials and Abstracts



European Microbeam Analysis Society

EMAS 2011

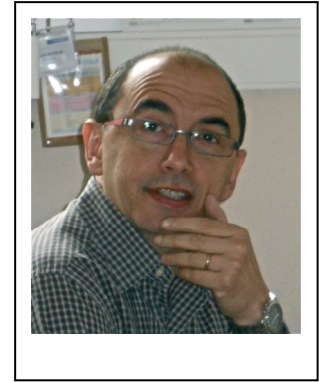
**12th
EUROPEAN WORKSHOP**

on

MODERN DEVELOPMENTS AND APPLICATIONS IN MICROBEAM ANALYSIS

**15 to 19 May 2011
at the
Centre de Congrès d'Angers
Angers, France**

Organised in collaboration with
GN-MEBA - Groupement National de Microscopie
Électronique à Balayage et de microAnalyses



NUCLEAR REACTION ANALYSIS (NRA) AT THE MICROMETRE SCALE

Hicham Khodja

C.E.A., Centre de Saclay, IRAMIS - Institut Rayonnement Matière de Saclay, SIS2M - Service Interdisciplinaire sur les Systèmes Moléculaires et les Matériaux, LEEL - Laboratoire d'Etude des Eléments Légers
FR-91191 Gif-sur-Yvette Cedex, France

and

C.N.R.S., UMR 3299, SIS2M - Service Interdisciplinaire sur les Systèmes Moléculaires et les Matériaux, LEEL - Laboratoire d'Etude des Eléments Légers
FR-91191 Gif-sur-Yvette Cedex, France
e-mail: hicham.khodja@cea.fr

Hicham Khodja was born in Bizerte, Tunisia on December 5, 1966. He received an M.Sc. degree in physics from the University of Grenoble in 1990, and the Ph.D. degree in physics from the University of Paris 6, Pierre et Marie Curie, in 1993. He joined the C.E.A./Grenoble where he worked on ECR plasma spectroscopy and modelling. In 1998, he moved to C.E.A./Saclay where he has worked on ion beam interactions with matter. He is currently head of the Laboratoire d'Etude des Eléments Légers (LEEL), part of the SIS2M C.E.A.-C.N.R.S. joint laboratory. He has published over 60 papers in refereed journals.

1. *ABSTRACT*

This article provides an overview of the nuclear reaction analysis technique when used with micrometric ion beams. After recalling the major principles underlying nuclear reaction processes in the context of analytical applications, we focus on the specific effects met when using microbeams. Numerous applications of nuclear reaction analysis can be found in the literature; some of them are described as an illustration of the capabilities of the technique.

2. *INTRODUCTION*

About half a century ago, S Rubin and colleagues [1] published the first paper reporting application of nuclear reactions induced with swift light ions for analytical purposes, giving the starting point of the nuclear reaction analysis technique (NRA), one of the pillars of the ion beam analysis (IBA) toolbox. Since that time, considerable progresses were made to push ahead the limits of this technique, with a specific emphasis on applications with microbeams, as modern low energy accelerators can be conveniently equipped with microbeam – in some cases sub-microbeam – lines. These facilities, called nuclear microprobes (NMP), are found all around the world and are used for various research fields, ranging from material science to biology. Today NRA is a convenient analytical option when beyond-surface or depth-resolved absolute light element measurements are required. In this review paper, we intend to give an overview of the technique in the current research context. An abundant review literature and handbooks related to NRA already exist [2-5], so our ambition here is to deliver some guidelines for those who might intend to use μ -NRA and are not familiar with. We will first briefly recall in section 3 some generalities about IBA, with a highlight on NRA. In section 4, we'll examine the particularities of NRA when performed with microbeams. Sections 5 to 7 are dedicated to some recent applications of NRA.

3. *PRINCIPLES OF NUCLEAR REACTION ANALYSIS*

NRA is part of the IBA set of techniques, that all rely on ion beam interactions with matter. A complete review of these interactions is beyond the scope of this paper, so we only recall here the principles and set out the guidelines governing ion beam interactions with matter. We also list IBA techniques, with emphasis on NRA. A common point between the different IBA techniques is that all of them are considered as quantitative methods, since all the physical stages giving rise to a particle or radiation detection are extremely well described and modelled for decades. Importantly, this allows standard-free measurements in most cases. A second common feature shared by IBA techniques is that all are insensitive to atom environment, thus producing speciation-independent measurements.

3.1. Ion beam interactions with matter

Swift charged particles interact with their environment mainly through electromagnetic interaction, leading to energy exchanges with neighbouring nuclei and electrons. This leads to a progressive slowing down of the incoming particle, until it stops in a potential well. Absorbed energy is essentially thermalized in the target, but a small part converted to potential energy through atomic displacements induced by ballistic collisions.

A standard way of evaluating this energy exchange is based on the energy loss concept that associate an energy loss rate with distance that depends on the projectile/target atom set:

$$\Delta E = \int_{E_0}^0 S(E) \quad \text{with} \quad S(E) = \frac{dE}{dx}(E) \quad (1)$$

with ΔE is the total energy loss, $S(E)$ is the energy loss rate (also called stopping power) and E_0 is the initial energy. Obviously, if the projectile comes at rest, $\Delta E = -E_0$. Elemental stopping power databases are regularly refined and evaluated. For compounds, a simple additive rule (Bragg rule) is applied at first approximation, i.e., for a A_mB_n molecule, the energy loss will be

$$\left(\frac{dE}{dx}\right)_{A_mB_n} = \left(\frac{m}{m+n}\right)\left(\frac{dE}{dx}\right)_A + \left(\frac{n}{m+n}\right)\left(\frac{dE}{dx}\right)_B$$

Range at which the incoming ions come at rest R in materials can be evaluated using stopping power data through the equation:

$$R = \int_{E_0}^0 \frac{1}{dE/dx} dE \quad (2)$$

Stopping power is generally presented as a two-component expression. First one is linked to projectile-electron Coulombian interaction, the other linked to projectile-nuclei Coulombian interaction:

$$\frac{dE}{dx} = \left.\frac{dE}{dx}\right|_{Nuc} + \left.\frac{dE}{dx}\right|_{Ele}$$

Subscripts *Nuc* and *Ele* refer to nuclear and electronic components. Analytical expressions of nuclear and electronic energy losses are available in the literature, derived from Bohr evaluations and where the key parameter is the ratio of projectile with electron velocities that drives the screening magnitude of the Coulombian interaction. Most refined expressions are known as Ziegler, Biersack and Littmark (ZBL) nuclear stopping power and Lindhard-Scharff (LS) electronic stopping power [6]. These analytical expressions are regularly compared with

experimental data and excellent agreements are found. The only observed discrepancy is linked with the use of the Bragg rule for organic materials, requiring correction factors obtained from experiments.

Considering light ion projectiles such as those employed for IBA, namely $^1\text{H}^+$, $^2\text{H}^+$ (or d), $^3\text{He}^+$ and $^4\text{He}^+$, it is observed that the major part of the energy is lost through ion-electron (inelastic) interactions, nuclear collisions becoming significant only at the very end of the path. This observation allows to consider IBA technique as a non-destructive technique, provided (i) beam induced heat is clearly evaluated and – if needed – minimized, (ii) charge neutralisation is established.

3.2. IBA techniques (except NRA)

3.2.1. PIXE

Surprisingly, the most popular ion beam technique used with nuclear microprobes is not linked to projectile-nucleus interaction but is related to electronic interaction. The proton induced X-ray emission technique (PIXE) is performed in all laboratories equipped with NMP. This is linked to the easy transposition of electron or photon based fluorescence probing, to the high inner-shell electron ionisation cross-sections (comparable to that produced with an electron with the same velocity) and to the relatively low background level owing to the inefficient Bremsstrahlung process when using ion projectiles instead of electrons. These particularities lead to limits of detection in the ppm range for a large array of elements.

3.2.2. RBS

The Rutherford backscattering (RBS) technique is the most classical one employed with ion beams, although limits of detection are high (typically 0.1 at%). In the context of NMP, it is generally used as a complementary technique to monitor the incoming flux and control the major element composition of the sample.

3.2.3. ERDA

Elastic recoil detection analysis (ERDA), based on the collection of light ejected recoil atoms during elastic collisions, is a convenient method for measuring very light elements in heavy matrixes. It requires however an unconventional geometry (grazing incidence), reducing lateral resolution and depth of the analysis. It is considered as one of the key techniques for hydrogen detection and quantitative evaluation.

3.3. NRA

Are considered relevant to NRA here all the interactions where a nuclear process is induced during the encounter between projectile and target. This covers Coulomb excitation, direct nuclear reactions and compound nucleus formation process. All these classes of reactions obey to general conservation rules, namely total energy conservation, charge conservation and total momentum conservation. Nuclear reactions are frequently written under the compact form $X(a,b)Y$, where X is the target atom, a the energetic projectile; b and Y are reaction products, where Y is the heavy atom, and b is the light product that is generally measured. A general layout of the reaction geometry is given in Fig. 1. If many light particles are observed, they are all indicated in the brackets: $^{19}\text{F}(p,\alpha\gamma)^{16}\text{O}$ denotes a nuclear reaction induced with protons on ^{19}F , producing a α - and γ -emissions and an ^{16}O residual nucleus.

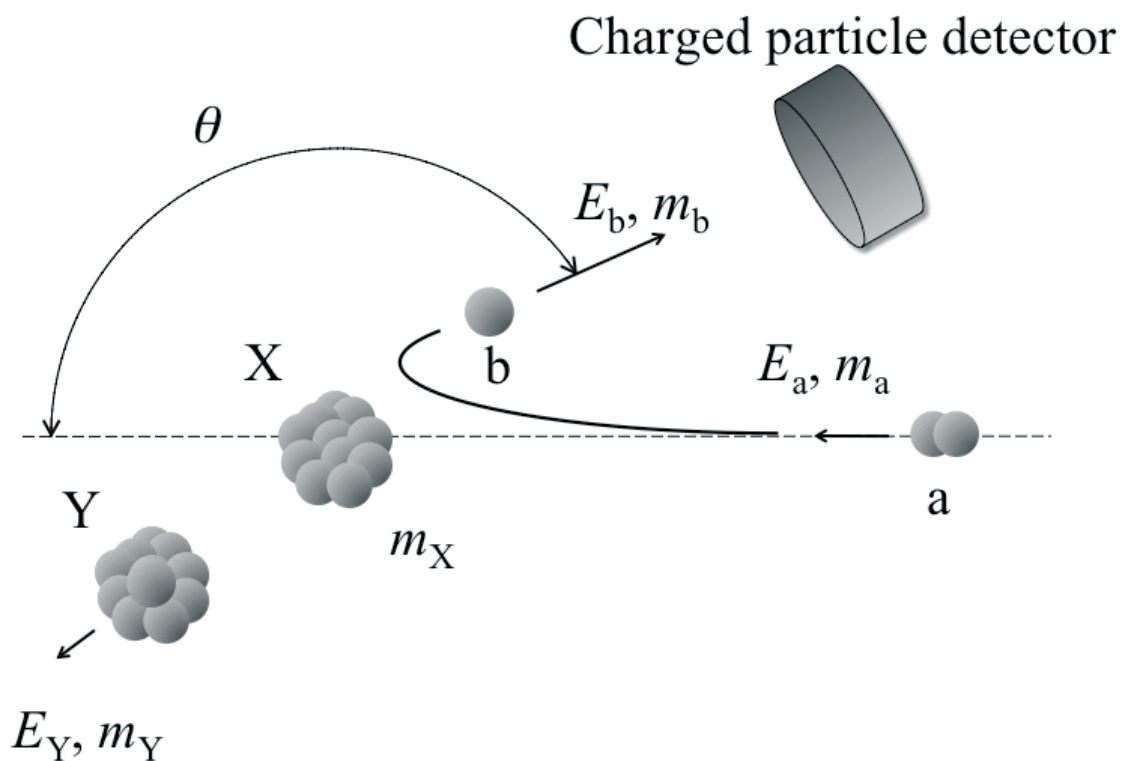


Figure 1. Schematic view of the typical $^{12}\text{C}(d,p)^{13}\text{C}$ nuclear reaction in NRA configuration.

Referring to the condensed nuclear reaction formulation, total energy conservation (including the mass energy) can be written in the form

$$T_a + Q = T_b + T_Y$$

with

$$Q = (m_a + m_X - m_b - m_Y)c^2$$

T and m being kinetic energies and masses of the different particles indicated in subscript. We suppose that the target X is at rest, which is always the case in analytical arrangements. The Q -value represents the kinetic energy excess of the final products, the mass difference originating from the nucleus binding energies. Similarly to classical chemical reactions, Q can be viewed as a heat of reaction, and depending on the sign, the reaction is said exo- (> 0) or endoenergetic (< 0). If the residual nucleus is produced in an excited state E_{ex} above ground state, than Q -value has to be lowered by E_{ex} in all equations.

A careful treatment of the kinematics demonstrates that in the case of endoenergetic reactions ($Q < 0$), reaction occurs only above a threshold higher than $(-Q)$. Its maximum value is reached for forward ($\theta = 0^\circ$) kinematics:

$$T_a^{\text{Thres.}} = -Q \frac{m_b + m_Y}{m_b + m_Y - m_a} \quad (3)$$

In analytical applications, nuclear reactions occur at variable energies as the incoming beam slows down during sample traversal, and as long as the reaction cross-section does not fall to zero. Moreover, energetic emitted particles also experience a slowing down along the path to the detector (Eq. (1)). This implies that generally there is an unambiguous relationship between detected particle energy and depth of reaction, thus giving access to depth resolution. There are also some specific nuclear reactions where cross-sections reach maximum values at very specific energies with narrow widths. By varying the incoming energy, these resonant nuclear reactions occur at variable depths, allowing also elemental depth profiling.

Coulomb excitation, or inelastic Coulomb scattering, is a process where energy transfer occurs through virtual photon exchange from projectile target nucleus. No nucleon redistribution occurs, as a fraction of the kinetic energy is absorbed by the target nucleus. Absorption leads to excited-state formation, which decays through prompt γ -ray emission. Table 1 lists some of the commonly used Coulomb excitation reactions for NRA.

Direct reaction process occurs when a projectile interact very rapidly ($\sim 10^{-22}$ s) with the target nucleus. The interaction volume is generally confined to peripheral nucleons. Two types of direct reactions are of interest for analysis purposes: stripping and pickup reactions. The first type refers to a removal of nucleons from the projectile, which is the case for (d,p) reactions. The second type corresponds to an interaction where the projectile captures nucleons from the target (e.g., (d, α) reactions). In Table 2 are listed some of the used direct reactions.

Table 1. Some useful Coulomb excitation nuclear reactions for elemental analysis. γ -ray yields are normalized per unit of deposited charge (μC) and solid angle (Sr).

Element	Nuclear reaction	γ -ray energy (keV)	γ -ray yield in thick target with 3.1 MeV protons (N/mC.Sr)
${}^7\text{Li}$	${}^7\text{Li}(p,p'\gamma){}^7\text{Li}$	478	$5.6 \cdot 10^7$
${}^{19}\text{F}$	${}^{19}\text{F}(p,p'\gamma){}^{19}\text{F}$	197	$2.0 \cdot 10^7$
${}^{24}\text{Mg}$	${}^{24}\text{Mg}(p,p'\gamma){}^{24}\text{Mg}$	1368	$9.3 \cdot 10^5$
${}^{25}\text{Mg}$	${}^{25}\text{Mg}(p,p'\gamma){}^{25}\text{Mg}$	585	$2.2 \cdot 10^5$
${}^{27}\text{Al}$	${}^{27}\text{Al}(p,p'\gamma){}^{27}\text{Al}$	1014	$4.6 \cdot 10^6$
${}^{31}\text{P}$	${}^{31}\text{P}(p,p'\gamma){}^{31}\text{P}$	1266	$1.6 \cdot 10^6$
${}^{35}\text{Cl}$	${}^{35}\text{Cl}(p,p'\gamma){}^{35}\text{Cl}$	1219	$2.2 \cdot 10^5$

Table 2. Some useful direct and compound-nucleus nuclear reactions for elemental analysis. The reaction occurs only above a certain threshold (Eq. (3)). The actual detected particle energy will also depend on the geometry and the energy loss in the foil used to absorb backscattered particles.

Direct reactions			Compound-nucleus reactions		
Element	Nuclear reaction	Q-value (keV)	Element	Nuclear reaction	Q-value (keV)
${}^2\text{H}$	${}^2\text{H}({}^3\text{He},p){}^4\text{He}$	18354	${}^7\text{Li}$	${}^7\text{Li}(p,\alpha){}^4\text{He}$	17347
${}^3\text{He}$	${}^3\text{He}(d,p){}^4\text{He}$	18354	${}^{11}\text{B}$	${}^{11}\text{B}(p,\alpha){}^8\text{Be}$	8591
${}^9\text{Be}$	${}^9\text{Be}(d,p){}^{10}\text{Be}$	4587	${}^{15}\text{N}$	${}^{15}\text{N}(p,\alpha){}^{12}\text{C}$	4966
${}^9\text{Be}$	${}^9\text{Be}({}^3\text{He},p){}^{11}\text{B}$	10323	${}^{18}\text{O}$	${}^{18}\text{O}(p,\alpha){}^{15}\text{O}$	3980
${}^{10}\text{B}$	${}^{10}\text{B}(d,p){}^{11}\text{B}$	9231	${}^{19}\text{F}$	${}^{19}\text{F}(p,\alpha){}^{16}\text{O}$	8115
${}^{10}\text{B}$	${}^{10}\text{B}(d,\alpha){}^8\text{Be}$	17822			
${}^{12}\text{C}$	${}^{12}\text{C}(d,p){}^{13}\text{C}$	2722			
${}^{13}\text{C}$	${}^{13}\text{C}(d,p){}^{14}\text{C}$	5952			
${}^{14}\text{N}$	${}^{14}\text{N}(d,p){}^{15}\text{N}$	8609			
${}^{14}\text{N}$	${}^{14}\text{N}(d,\alpha){}^{12}\text{C}$	13575			
${}^{16}\text{O}$	${}^{16}\text{O}(d,p){}^{17}\text{O}$	1918			
${}^{28}\text{Si}$	${}^{28}\text{Si}(d,p){}^{29}\text{Si}$	6249			

Compound nucleus formation is a process where the projectile interacts with a nucleus at small impact parameters, and energy is first transferred to a bounded nucleon and then “thermalized” to other nucleons. The formed compound nucleus then decays by fragment emission, which is

generally a light nucleus. Importantly, as transferred energy is nearly randomly shared among nucleons, emitted particle angular distribution is nearly isotropic, in contrast with direct process where strong angular dependence characterizes angular distributions. Some of the reactions with analytical use are listed in Table 2. As the compound nucleus formation is a multistep process, reaction times are typically of the order of 10^{-18} s.

Differential cross-section, that estimates probability of interaction, is a parameter that is highly contrasted from one reaction to another and is also frequently highly anisotropic due to the quantum nature of nuclear reactions. It contrasts with the classical Coulomb elastic scattering process, where the analytical Rutherford cross-section formula expression, experimentally relevant for a large set of projectiles and nuclei, show a smooth dependency with parameters such as energy, angles, charges and masses. In most cases, NRA differential cross-sections are low (the highest NRA cross-section is 110 mb/Sr for the $^{12}\text{C}(\text{d,p})^{13}\text{C}$ reaction, to be compared to 3.5 b/Sr for the $^{56}\text{Fe}(\alpha,\alpha)^{56}\text{Fe}$ RBS at 1 MeV, or 1.73 b/Sr Fe X-ray production with 3 MeV protons). The consequences are that detection limits are rarely better than 0.01 wt%, and if statistical precision is required, acquisition times can be considerably long.

Resonance reactions are particular nuclear reactions, where cross-sections present sharp maxima at discrete energies. This may occur when the transferred energy matches one of the discrete energy levels of the intermediate compound nucleus. Ideally, a nuclear reaction with a single sharp resonance offers a very convenient way of depth profiling. By varying the incoming energy beam, the reaction probes different depths of the sample with direct access to the concentration depth profile. In Table 3 we list some of the most used resonances. When possible, it is very interesting to detect g-rays resulting from the resonant reaction instead of the charged particles, as photons do not experience energy scattering resulting in a loss of resolution. Moreover, it is possible for some situations to use very large detectors that optimize statistics. It is typically the case for the $^1\text{H}(^{15}\text{N},\alpha\gamma)^{12}\text{C}$ reaction where very large area gamma detectors are available. With such an optimal configuration, it is possible to discriminate hydrogen presence with atomic monolayer resolution [7].

4. NRA AT THE MICROMETRE SCALE

Nuclear reaction analysis was used and developed before emergence and routine use of the microbeam technique. Thus the magnitude of local damage induced by high current densities and very long beam exposures were not initially examined. A classical interrogation before NRA experiments is the potential heating of the sample induced by microbeam energy deposition. Actually, it is demonstrated that for steady ion currents, no significant heating is induced with standard microbeam parameters [8]. Classical heat transfer equations show that a 2 MeV, 1 nA, 5 mm² deuteron beam impacting on a glass sample induces a moderate temperature elevation locally evaluated to 50 K. More difficult to grasp, unstable ion currents

Table 3. Nuclear resonances useful for light element depth profiling. Small resonance widths Γ denote a high depth profiling potency.

Element	Nuclear reaction	E (MeV)	Γ (keV)
^1H	$^1\text{H}(^{15}\text{N},\alpha\gamma)^{12}\text{C}$	6.385	1.8
^{15}N	$^{15}\text{N}(\text{p},\alpha\gamma)^{12}\text{C}$	0.429	0.12
^{18}O	$^{18}\text{O}(\text{p},\alpha)^{15}\text{O}$	0.152	0.05
^{18}O	$^{18}\text{O}(\text{p},\alpha)^{15}\text{O}$	0.633	2.0
^{19}F	$^{19}\text{F}(\text{p},\alpha\gamma)^{16}\text{O}$	0.872	4.5
^{27}Al	$^{27}\text{Al}(\text{p},\gamma)^{16}\text{O}$	0.992	0.03

can induce high temperature excursions, particularly in the beam impact volume where noise heating dominates [9]. If necessary, when high mobility species are present, a moderate cooling of the sample is performed.

The second type of damage that can be induced by NRA exposure conditions is the ballistic displacement of atoms, particularly at the end of the path where nuclear collisions become relatively important. The damage mechanism consists in a kinetic energy transfer to an atom, leading to a displacement in a vacancy or interstitial position in the crystallographic structure. The energy transfer has to be above a certain threshold to induce an effective displacement. Order of magnitude of thresholds is in the range of 10 - 30 eV [6]. Here, damages will be directly proportional to charge density, and thus exposure times. A convenient way for estimating ballistic damage is to use SRIM software [10]. With the same beam parameters as above, a 0.1 μm deposited charge generates on glass 0.3 displacements per atom on average along the path (here conservatively considered as a straight cylinder), but are sharply concentrated around the implantation area. It should be noted however that this value indicates the fraction of target atoms experiencing a displacement independently from their final locations (substitutional or interstitial). Thus it represents an upper limit for sample structural damage. Moreover, as displacements are mainly concentrated at the end of the path, no significant impact is expected on NRA analysis as cross-sections fall to zero before incoming ions come at rest. It points out however how sub-micrometre beams can induce significant damages if similar fluences are used. The best strategy is probably to develop new NRA setups with optimized solid angle configurations and high data flux capabilities.

A last side effect that should be considered when performing $\mu\text{-NRA}$ is the transmutation induced by nuclear reactions. Still considering above beam parameters, but here impinging on a pure carbon target (the $^{12}\text{C}(\text{d},\text{p})^{13}\text{C}$ nuclear reaction has one the highest NRA cross-section), a rough calculation predicts that less than 0.5 % of the total ^{12}C atoms will be transmuted. Consequently, this effect can be considered as negligible.

5. APPLICATIONS TO MATERIAL SCIENCE

Material science is currently the field of research that makes the most intensive use of the NRA technique. This is probably linked to the relative lack of techniques for quantitative evaluation of light elements in solid matrixes. It is possible to classify these studies in three categories: electronic-related materials, nuclear materials and technological materials. Although an exhaustive list of applications in material science is beyond the scope of the article, we present here some recent studies based on NRA.

Electronic-related material research develops new semiconductors using innovative materials and processes, generating a huge demand for characterisations. In particular, atomic concentrations, layer thicknesses and interdiffusion profiles can be of major importance regarding expected properties. For example, boron-doped germanium is an attractive candidate for future microelectronics thanks to its remarkable transport properties. In this frame, fluences of boron implanted at 100 nm depth in Ge were precisely evaluated using the $^{11}\text{B}(p,\alpha)^8\text{Be}$ reaction at 650 keV [11]. TaC_xN_y thin films are currently investigated for various applications in microelectronics. Thin film composition depends strongly on the deposition methods and parameters and N/Ta and C/Ta were precisely evaluated by combination of $^{12}\text{C}(d,p)^{13}\text{C}$ – $^{14}\text{N}(d,p)^{15}\text{N}$ with Ta RBS measurements [12]. Metal-oxide-semiconductor devices based on silicon carbide are proposed for applications under extreme conditions. Using isotope labelling, Soares and colleagues [13] have recently investigated hydrogen incorporation during SiO_2 thermal growth under isotopically-enriched vapour atmosphere. Using the depth-resolved $^2\text{H}(^3\text{He},p)^4\text{He}$ nuclear reaction authors demonstrated that hydrogen profile depends on substrate type. Annealing effects on N-concentration in GaAsN [14] were recently evaluated using $^{14}\text{N}(d,p)^{15}\text{N}$ and $^{14}\text{N}(d,\alpha)^{12}\text{C}$ nuclear reactions. Ultra-shallow implantation needs to be highly mastered in view of ultra-large scale integration. Tomita *et al.* [15] combined NRA and SIMS techniques to estimate precisely junction depths and doses of low energy implanted boron on SiGe surfaces. It is worth noting that lateral resolution is rarely useful for this type of studies, as minimal usable beam size is generally wider than structural dimensions. Depth resolution, frequently lower than 100 nm with NRA, is however a great advantage of this technique in this context.

Light element behaviour in nuclear materials is a very important aspect that has a strong impact on material properties during its lifecycle, i.e., mechanical properties that impact safety during reactor operation or confinement capabilities during fuel storage. Here a number of studies are devoted to hydrogen accumulation and distribution in cladding materials [16], radiogenic helium release and behaviour in radioactive fuel [17]. μ -NRA is here well suited for these studies as object sizes fall in the millimetre range. Another significant use of μ -NRA with nuclear materials is associated to fusion-related materials. Of crucial importance, tritium deposition and retention that occur during plasma discharges are considered as key features for future tokamak plasma facing component (PFC) designs. Here μ -NRA is extremely helpful

since elemental balance is of primary importance. It is applied to materials exposed to deuterium ion beams or plasmas [18, 19], thus combining lateral and depth resolutions, and offers an excellent investigation tool for anticipating PFC material behaviour for long term plasma discharge operation.

NRA is also applied to technological materials, particularly through non-radioactive isotopic labelling technique. As an illustration, oxidation processes using deuterium or ^{18}O labelling [20] and growth mode of carbon nano-tubes using ^{13}C [21] were investigated using μ -NRA. It allowed reconstructing reaction chronologies thus helping in identifying oxidation or growth mechanisms.

6. *APPLICATIONS TO EARTH AND PLANETARY SCIENCE*

Earth and planetary science researchers constitute also an important user community of NRA at the micrometre scale. Indeed, multiphasic, micrometre-scale objects found in rocks are frequently investigated in this field. They are both natural and synthetic, and help in exploring the thermodynamic conditions found in magmatic extreme conditions. CO_2 in fluid and gas inclusions hosted in olivine is a witness of thermodynamic conditions of inclusion formation. Consequently carbon concentration in inclusions helps in understanding magma formation and dynamics during eruption events [22, 23]. μ -NRA is also successfully applied to invaluable micrometre cometary grains collected by the Stardust NASA mission. C and N light elements are of primary importance for numerous reasons, among them determination of redox conditions for comet formation and extraterrestrial C and N introductions in earth atmosphere during initial cometary bombardment. Here a grain-by-grain analysis using deuteron based nuclear reactions allowed absolute evaluations of C and N contents [24]. Standard NRA is also employed in earth and planetary science helping in determination of diffusion properties of light elements as He and Li in mineral matrixes [25, 26].

7. *OTHER APPLICATIONS*

Samples originating from cultural heritage and environment/pollution fields cannot usually handled as standard samples. In particular, the size and/or the great number of these objects exclude in-vacuum analyses. Instead of performing charged-particle emission spectroscopy, γ -ray emission spectroscopy offers an efficient method for light element evaluation in such conditions. Although not strictly considered as an NRA sub-technique, particle induced gamma-ray emission (PIGE) is also based on nuclear processes. It is particularly well suited for elements such as ^{19}F , ^{23}Na or ^{40}Ca (see Table 1 and [27, 28]). This method is frequently employed in conjunction with PIXE for micro/macro analysis of such samples [29-31].

8. CONCLUSIONS

μ -NRA is probably the technique that is the most specific to nuclear microprobes, since all other available IBA techniques have strong similarities with few other popular analytical techniques (X-ray emission with SEM and X-ray tubes, particle scattering with medium energy ion scattering devices (MEIS), particle recoil analysis with SIMS, ...). The main drawback is a relatively weak detection limit that can be sorely compensated by long time exposures generating ballistic damages with high-current microbeams. However, with some precautions, it offers a convenient method for non-destructive light element quantitative analysis at the micrometre scale, with isotopic sensitivity and is not limited to surface analysis thanks to the inherent high-energy processes. In frequent situations, it also allows depth resolved analyses with a 10 - 100 nm resolution. Used with complementary techniques, μ -NRA helps investigating different processes implying light elements and is well adapted for various fields, and particularly material science.

9. REFERENCES

- [1] Rubin S, Passell T O and Bailey L E (1957) *Anal. Chem.* **29**: 736-743.
- [2] Demortier G (1995) *Nucl. Instrum. Methods Phys. Res. B* **104**: 244-254.
- [3] Trocellier P, Berger P, Berthier B, Berthoumieux E, Gallien J, Metrich N, Moreau C, Mosbah M and Varela M (1999) *Nucl. Instrum. Methods Phys. Res. B* **158**: 221-227.
- [4] Tesmer J R and Nastasi M A (1995) *Handbook of modern ion beam materials analysis*. Materials Research Society Handbook (Materials Research Society, Pittsburgh).
- [5] Trocellier P and Berger P (2009) *Nuclear reaction spectroscopy encyclopedia of analytical chemistry* (Meyers R A, Ed.) John Wiley & Sons, Ltd (Chichester, UK).
- [6] Nastasi M A, Mayer J W and Hirvonen J K (1996) *Ion-solid interactions: fundamentals and applications*. Cambridge University Press (Cambridge).
- [7] Wilde M, Fukutani K, Naschitzki M and Freund H (2008) *Phys. Rev. B* **77**: 113412.
- [8] Plumereau G, Ailloud P, Berger P, Boutard D, Guittet J-M and Ladieu F (1999) *Nucl. Instrum. Methods Phys. Res. B* **149**: 153-166.
- [9] Plumereau G, Aranda P, Ailloud P, Berger P, Boutard D and Ladieu F (1999) *J. Appl. Phys.* **85**: 134.
- [10] Ziegler J F, Ziegler M and Biersack J (2010) *Nucl. Instrum. Methods Phys. Res. B* **268**: 1818-1823.
- [11] Mirabella S, Impellizzeri G, Piro A, Bruno E and Grimaldi M (2008) *Appl. Phys. Lett.* **92**: 251908.
- [12] Anacleto A C, Zauner A, Cany-Canian D, Gatineau J and Hugon M (2010) *Thin Solid Films* **519**: 367-372.
- [13] Soares G V, Baumvol I J R, Correa S A, Radtke C and Stedile F C (2010) *Electrochem. Solid St.* **13**: G95-G97.

- [14] Jin Y, Jock R M, Cheng H, He Y, Mintarov A M, Wang Y, Kurdak C, Merz J L and Goldman R S (2009) *Appl. Phys. Lett.* **95** 062109.
- [15] Tomita M, Suzuki M, Tachibe T, Kozuka S and Murakoshi A (2003) *Appl. Surf. Sci.* **203-204**: 377-382.
- [16] Raepsaet C, Bossis P, Hamon D, Bechade J and Brachet J (2008) *Nucl. Instrum. Methods Phys. Res. B* **266**: 2424-2428.
- [17] Pipon Y, Raepsaet C, Roudil D and Khodja H (2009) *Nucl. Instrum. Methods Phys. Res. B* **267**: 2250-2254.
- [18] Petersson P, Kreter A, Possnert G and Rubel M (2010) *Nucl. Instrum. Methods Phys. Res. B* **268**: 1833-1837.
- [19] Wright G, Alves E, Alves L, Barradas N, Carvalho P, Mateus R and Rapp J (2010) *Nucl. Fusion* **50**: 055004.
- [20] Chitty W, Berger P, Dillmann P and Lhostis V (2008) *Corros. Sci.* **50**: 2117-2123.
- [21] Pinault M, Pichot V, Khodja H, Launois P, Reynaud C and Mayne-L'Hermite M (2005) *Nano Lett.* **5**: 2394-2398.
- [22] Spilliaert N, Allard P, Métrich N and Sobolev A V (2006) *J. Geophys. Res.* **111**: B04203.
- [23] Metrich N, Bertagnini A and Di Muro A (2010) *J. Petrol.* **51**: 603-626.
- [24] Gallien J *et al.* (2008) *Meteorit. Planet. Sci.* **43**: 335-351.
- [25] Cherniak D, Watson E and Thomas J (2009) *Chem. Geol.* **268**: 155-166.
- [26] Cherniak D J and Watson E B (2010) *Contrib. Mineral Petrol.* **160**: 383-390.
- [27] Mateus R, Jesus A P and Ribeiro J P (2004) *Nucl. Instrum. Methods Phys. Res. B* **219-220**: 519-523.
- [28] Dherendra G and Peisach M (1991) *Elemental analysis by particle accelerators* (Alfassi Z B and Peisach M, Eds.) CRC Press (Boca Raton): 307-348.
- [29] Calligaro T, Dran J, Salomon J and Walter P (2004) *Nucl. Instrum. Methods Phys. Res. B* **226**: 29-37.
- [30] Demortier G and Nammour S (2008) *Nucl. Instrum. Methods Phys. Res. B* **266** : 2408-2411.
- [31] Giuntini L, Massi M and Calusi S (2007) *Nucl. Instrum. Methods Phys. Res. B* **576**: 266-273.